Synthesised H_∞ / μ Control Design for Dynamically Substructured Systems

T Yamaguchi[1,2] and D P Stoten[1]

[1]Advanced Control and Test Laboratory (ACTLab), Department of Mechanical Engineering, University of Bristol, Bristol BS8 1TR, UK
[2] Running Gear Laboratory, Vehicle Structure Technology Division, Railway Technical Research Institute, Tokyo 185-8540, Japan

E-mail: yamaguchi.teruya.30@rtri.or.jp

Abstract. In the dynamically substructured system (DSS) testing technique, a controller that synchronises the responses of physical and numerical substructures is an essential part of the testing scheme to ensure synchronisation fidelity. This paper discusses a novel approach that generates a two-degree-of-freedom (2-DOF) output feedback controller for multi-input, multi-output (MIMO) DSS via control synthesis. This 2-DOF output feedback controller yields robust stability and robust performance of the physical/numerical substructure synchronisation and enables controller tuning in the frequency domain. Simulation and experimental results have been shown to validate the efficacy of the method.

1. Introduction

The dynamically substructured system (DSS) approach [1] is a testing technique that combines full-size physical components (physical substructure) with a real-time numerical simulation of the remaining components (numerical substructure) in order to replicate the dynamical behaviour of a complete (or emulated) system. One of the main advantages of this technique is that the necessity and associated expense of constructing a complete physical system is avoidable. In addition, the full-size physical components will often contain unknown and nonlinear dynamics that would otherwise be difficult to model with sufficient accuracy. The concept of this type of testing was first proposed as hardware-in-the-loop simulation (HiLS) and hybrid simulation (HS), which have been implemented in various fields including the railway industry [2, 3, 4]. Whatever the method that is ultimately used, high-quality control is required to synchronise the responses of the physical and numerical systems at the interfaces between the two systems, in order to ensure the fidelity of the tests. In this respect, both the HiLS and HS approaches have been shown to offer poor stability and robustness, especially when the emulated system has low damping and/or pure-delay components [5].

The methodology of DSS and its control synthesis was first proposed by Stoten and Hyde [1], and was later extended via a state-space approach [6]. It has been shown that DSS provides significant stability and robustness compared with the more conventional approaches of HiLS and HS [5, 7]. A principle of the existing DSS approach is to design feedforward (FF) and feedback (FB) controllers that will realise the synchronisation objective. In this approach, the FF controller is partly formed via the inverse of the actuator dynamics in the physical substructure. Hence, it can be difficult to derive the FF controller for DSS actuator systems that possess high relative degree, multi-input, multi-output

(MIMO) dynamics or non-minimum phase dynamics. In addition, there is no requirement *per se* for a systematic design process for the FB controller (and a state observer, if necessary) to achieve the required synchronisation performance. Thus, the new H_∞ / μ control synthesis method for DSS (called H_∞ / μ-DSS), which is presented in this paper, is primarily motivated by these observations.

The novelty and main advantage of this new method is that it is unnecessary to design the FF controller and the state observer explicitly; *c.f.* [6]. Instead, the FF controller and the state observer are automatically synthesised by integrating the FB controller into a single system that is derived by H_∞ / μ control synthesis [8], in order to satisfy the main objective of synchronised substructure responses.

The rest of this paper is structured as follows. In §2, the H_∞ / μ-DSS approach is described in detail, where advantages of the method and its robust stability/performance are presented. In order to validate the efficacy of the method, experimental studies are presented in §3. Finally, the main conclusions of this work are presented in §4, including a brief description of an application to a railway testing facility, as a part of our future work in this field.

2. Synthesised H_∞/μ control design for DSS

2.1. Structure of the conventional DSS

A block representation of the state-space-based DSS is shown in Figure 1. Here, the physical substructure, Σ_P, typically consists of tested specimens, sensors and actuators. The numerical substructure, Σ_N, is usually a real-time simulation which computes the behaviour of the remaining components. The system excitation, d, is an external input to the DSS, $\{z_N, z_P\}$ are the outputs of $\{\Sigma_N, \Sigma_P\}$, y is the interaction constraint between the two substructures and the synchronising control signal, u, ensures that the synchronising error, z, is driven towards zero under all circumstances.

In the following developments, Σ_P and Σ_N are assumed to be linear systems, and the signals $\{d, u, y, z_N, z_P, z\}$ are, in general, vector quantities.

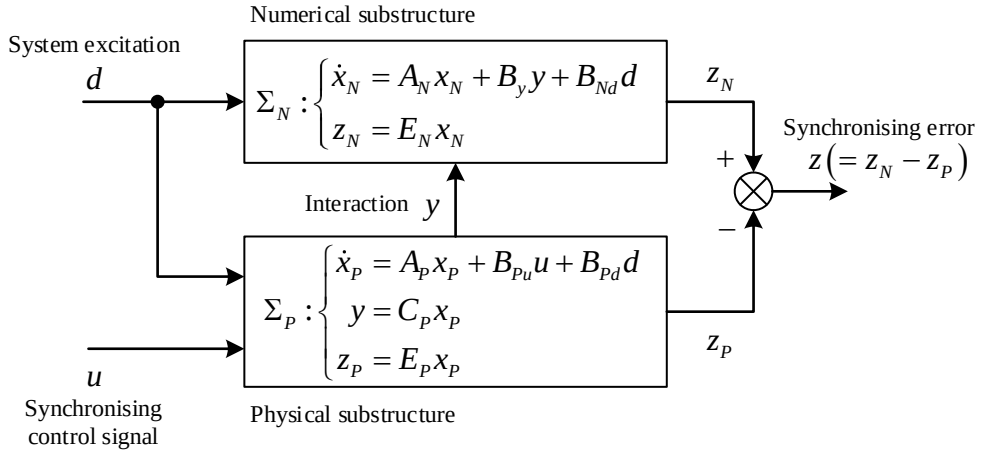

Figure 1. State-space-based DSS.

According to existing DSS theory, the controller consists of a FF term, K_d, and a FB term, K_e, as depicted in Figure 2. As discussed in §1, a proper realisation of the FF controller can be difficult to achieve in some cases. In order to address this issue and to employ the benefits of H_∞ / μ control synthesis, Σ_P / Σ_N and K_d / K_e are combined into a single dynamic system, as shown in §2.2.

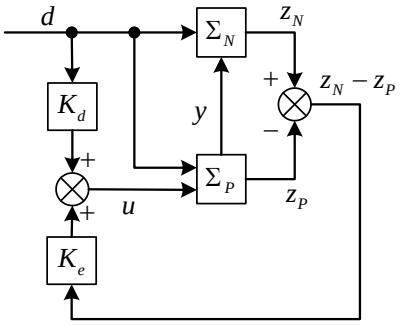

Figure 2. Structure of the standard DSS controller [1].

2.2. The generalised plant for DSS

The first step in the new approach is to transform the block representation in Figure 2 into the form shown in Figure 3, where Σ_C is referred to as the generalised plant in H_∞ / μ control theory. Note that the controller, K, has the form of a two-degree-of-freedom (2-DOF) output-feedback controller.

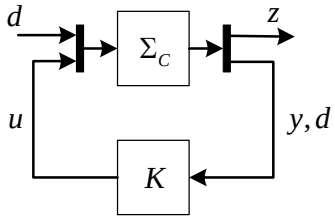

Figure 3. Generalised plant of DSS.

Σ_C can be expressed as

$$\Sigma_C : \left\{ \begin{array}{l} \dot{x}_C = A_C x_C + B_{Cu} u + B_{Cd} d \\ y = C_C x_C \\ z = E_C x_C \end{array} \right\} \tag{1}$$

where:

$$\left\{ \begin{array}{l} x_C = \begin{bmatrix} x_N \\ x_P \end{bmatrix} \\ A_C = \begin{bmatrix} A_N & B_y C_P \\ 0 & A_P \end{bmatrix},\ B_{Cu} = \begin{bmatrix} 0 \\ B_{Pu} \end{bmatrix},\ B_{Cd} = \begin{bmatrix} B_{Nd} \\ B_{Pd} \end{bmatrix} \\ C_C = \begin{bmatrix} I & C_P \end{bmatrix} \\ E_C = \begin{bmatrix} E_N & -E_P \end{bmatrix} \end{array} \right\} \tag{2}$$

Once the generalised plant is obtained, the existing H_∞ / μ control synthesis can be applied to derive the controller K, thus incorporating its advantageous features of frequency shaping, stability and robustness performance. Introducing an appropriately chosen weighting function, the following performance measures can then be attributed to the DSS design:

- Robust stability
- Nominal performance
- Robust performance

Here, the term 'robust' implies that the desired performance characteristics are ensured for all the possible uncertainties that are estimated within the design process. In the following sections, each of these performance characteristics are described in more detail.

2.2.1. Robust stability. Introducing the additive model uncertainty and perturbed system $\tilde{\Sigma}_C$, which can be expressed using transfer function matrices as follows:

$$\tilde{\Sigma}_C(s) = \Sigma_C(s) + \Delta(s)W_\Delta(s), \quad \|\Delta\|_\infty \le 1 \tag{3}$$

where $W_\Delta(s)$ is a weighting function that determines the frequency characteristics of the uncertainty and $\Delta(s)$ is a normalised and stable perturbation. The corresponding perturbed DSS is shown in Figure 4.

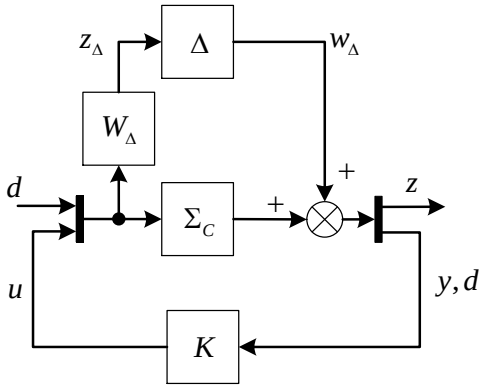

Figure 4. Perturbed DSS (additive perturbation).

In this case, according to the small gain theorem [8], the perturbed DSS is robustly stable for any $\Delta(s)$ if and only if

$$\|M_{z\Delta,w\Delta}\|_\infty < 1 \tag{4}$$

where $M_{z\Delta,w\Delta}(s)$ is the transfer function matrix from w_Δ to z_Δ in Figure 4. Alternatively, when the uncertainty within the system $\tilde{\Sigma}_C$ is modelled as a multiplicative term, i.e.:

$$\tilde{\Sigma}_C(s) = \Sigma_C(s)\{1 + \Delta(s)W(s)\}, \quad \|\Delta\|_\infty \le 1 \tag{5}$$

the perturbed DSS is as shown in Figure 5. Again, the perturbed DSS is robustly stable if and only if

$$\|M_{z\Delta,w\Delta}\|_\infty < 1 \tag{6}$$

where $M_{z\Delta,w\Delta}(s)$ is the redefined transfer function matrix from w_Δ to z_Δ in Figure 5. The γ iteration of H_∞-synthesis [9] enables the computation of a controller K that minimises $\|M_{z\Delta,w\Delta}\|_\infty$ so that the conditions in (4) or (6) can be satisfied.

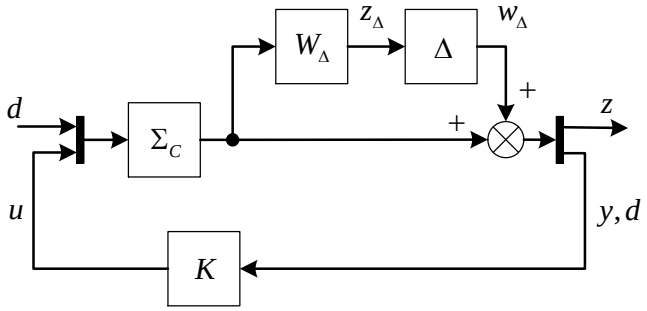

Figure 5. Perturbed DSS (multiplicative perturbation).

2.2.2. Nominal performance. Consider the DSS structure depicted in Figure 6. Choosing an appropriate weighting function, $W_z(s)$, defines the nominal performance as $\|M_{\bar{z},d}\|_\infty$, where $M_{\bar{z},d}(s)$ is the transfer function matrix from d to $\bar{z}$ in Figure 6.

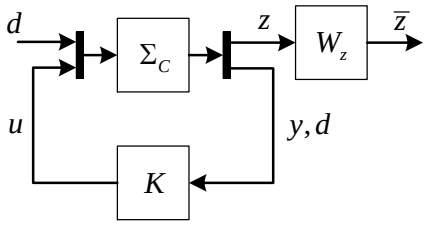

Figure 6. Nominal performance of DSS.

Again, the γ iteration can be used to minimise $\|M_{\bar{z},d}\|_\infty$, where the minimum value gives the nominal performance in the sense of an H_∞ norm. In addition, the condition $\|M_{\bar{z},d}\|_\infty < \gamma$, for a certain positive constant, γ, equates to the stability and robustness of the closed-loop system in Figure 7 in the presence of fictitious perturbation, Δ_f, such that $\|\Delta_f\|_\infty \le 1/\gamma$. This observation aids the discussion on robust performance in the next section.

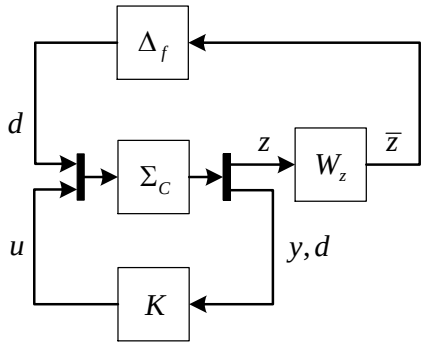

Figure 7. Equivalent expression of nominal performance.

2.2.3. Robust performance. Now consider the DSS structure shown in Figure 8, where the controlled plant is modelled as an additive uncertain model set. Using the development within the previous section, the perturbed system displays the robust stability and performance:

$$\|M_{\bar{z},d}\|_\infty < 1, \ \forall \Delta(s) \text{ s.t. } \|\Delta\|_\infty \le 1 \tag{7}$$

if

$$\left\| M_{\bar{z}z\Delta,dw\Delta} \right\|_\infty < 1 \tag{8}$$

where $M_{\bar{z},d}(s)$ is the redefined transfer function matrix from d to $\bar{z}$ and $M_{\bar{z}z\Delta,dw\Delta}(s)$ is the transfer function matrix from (d, w_Δ) to $(\bar{z}, z_\Delta)$ of the closed system in Figure 8.

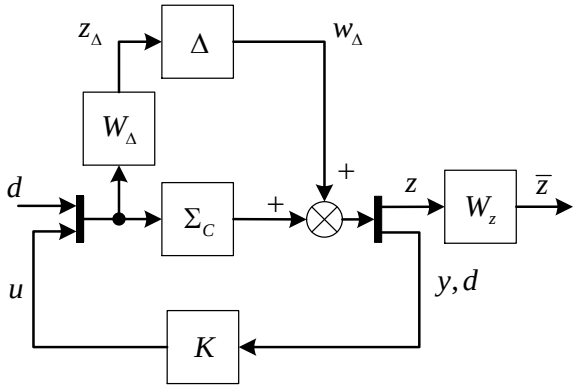

Figure 8. Robust performance of the DSS.

Introducing a fictitious perturbation, Δ_f, $\|\Delta_f\|_\infty \le 1$, the robust performance in (7) is identical to the robust stability of the closed-loop system shown in Figure 9.

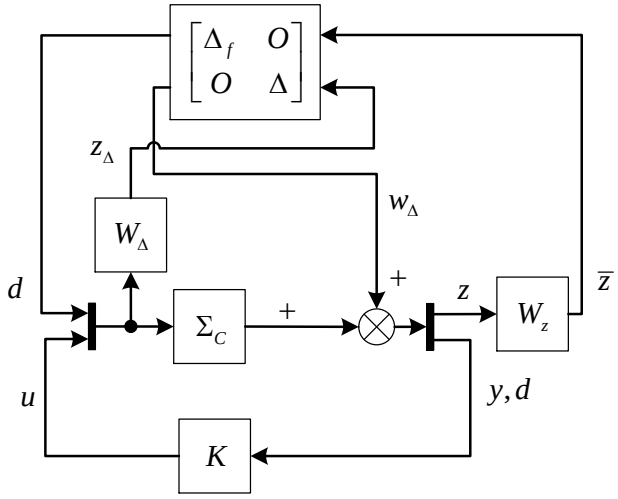

Figure 9. Equivalent expression of robust performance.

The condition in (7) can be derived from the following:

$$\left\| \Delta_P \right\|_\infty \triangleq \left\| \begin{bmatrix} \Delta_f & O \\ O & \Delta \end{bmatrix} \right\|_\infty \le 1 \tag{9}$$

Note that (9) only constitutes a sufficient condition to achieve robust performance. Hence a controller, K, that satisfies (9) can be quite conservative, a result induced by neglecting the structure of $\Delta_P(s)$. In order to overcome this problem, μ-synthesis was applied to the H_∞ / μ-DSS design. Thus, the

condition of the robust performance of the closed system in Figure 8 can be expressed as the following necessary and sufficient condition [9]:

$$\sup_{\omega\in\mathbb{R}} \mu_{\Delta_P}\left(M_{\bar{z}z\Delta,dw\Delta}(j\omega)\right)\leq 1 \tag{10}$$

where $\mu_{\Delta_P}(\bullet)$ is a structured singular value. The D-K iteration algorithm within the μ-synthesis procedure enables us to compute a controller K that minimises $\sup_{\omega\in\mathbb{R}} \mu_{\Delta_P}\left(M_{\bar{z}z\Delta,dw\Delta}(j\omega)\right)$, so that it satisfies the condition in (10). Such a controller ensures robust performance in (7) and to illustrate this feature, an experimental verification was conducted, details of which are given in §3. The overall scheme is shown in the block diagram of Figure 10.

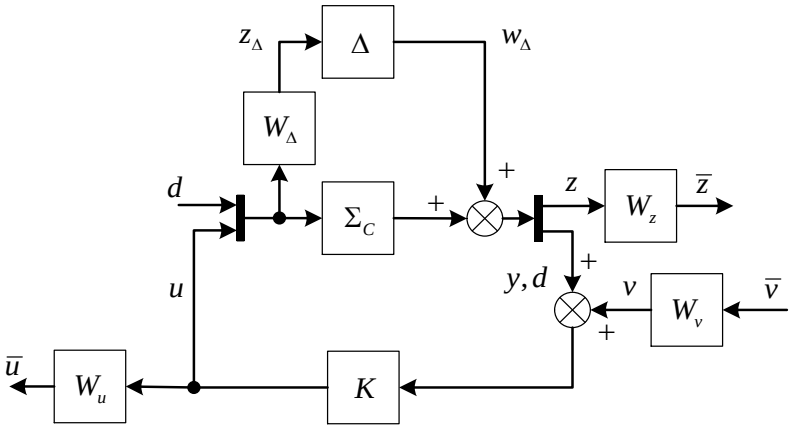

Figure 10. Robust performance of DSS in a practical situation.

Now redefine Δ_P as

$$\|\Delta_P\|_\infty \triangleq \left\| \begin{bmatrix} \begin{bmatrix} \Delta_{f11} & \Delta_{f12} \\ \Delta_{f21} & \Delta_{f22} \end{bmatrix} & O \\ O & \Delta \end{bmatrix} \right\|_\infty \leq 1 \tag{11}$$

and define the transfer function matrix $M_{\bar{z}\bar{u}z\Delta,d\bar{v}w\Delta}(s)$ relating $(d,\bar{v},w_\Delta)$ to $(\bar{z},\bar{u},z_\Delta)$ in Figure 10. Hence, under the assumption that the following condition is satisfied:

$$\sup_{\omega\in\mathbb{R}} \mu_{\Delta_P}\left(M_{\bar{z}\bar{u}z\Delta,d\bar{v}w\Delta}(j\omega)\right)\leq 1 \tag{12}$$

the system is robustly stable. In addition, the following robust performance:

$$\|M_{\bar{z}\bar{u},d\bar{v}}\|_\infty < 1,\ \forall\Delta(s)\ \text{s.t.}\ \|\Delta\|_\infty \leq 1 \tag{13}$$

is ensured, where $M_{\bar{z}\bar{u},d\bar{v}}(s)$ is the transfer function matrix from $(d,\bar{v})$ to $(\bar{z},\bar{u})$ of the closed-loop system in Figure 10.

Using this approach, the H_∞/μ-DSS scheme was further improved in terms of its practical application. In particular, if there is *a priori* knowledge of the model uncertainty and perturbations (i.e. observation noise and external disturbances) within the DSS, a controller can be designed that ensures robust stability and robust performance. In addition, degradation of control performance can be analysed when test specimens, actuators or numerical elements are changed. This can be of significant practical benefit, since additional system identification and control design can be avoided if satisfactory control performance can be guaranteed under such circumstances.

3. Experimental study

In order to verify the effectiveness of the new approach to DSS controller design, the following experiment was conducted. Firstly, the DSS structure and control specifications were defined. Secondly, system identification of the physical substructure was conducted and as a result, a DSS controller was designed via the new method. Finally, the desired performance specification was confirmed to be satisfied in the experiments.

3.1. Test rig and DSS specification

Figure 11(a) shows the electrical actuator for the experiment, consisting of an AC servo motor and a ball screw. As depicted in Figure 11(b), the servo driver enables the control of the motor velocity by a configurable in-built proportional-integral (PI) controller. In addition, a strain gauge was attached to a supporting rod of the actuator in order to measure the force that is applied by the external environment to the actuator.

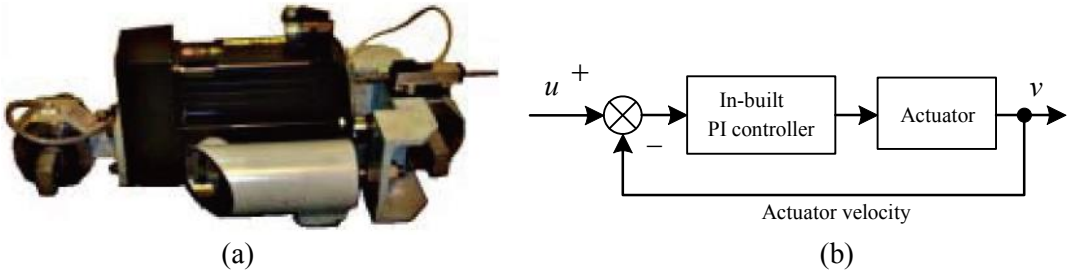

Figure 11. (a) AC actuator; (b) block schematic diagram of the electric actuator.

A schematic representation of the corresponding DSS test is shown in Figure 12. Here, the numerical substructure consists of a simple mass–spring–damper system, which is to be emulated by the actuator. The system excitation d is supposed to be the force that is measured by the strain gauge. The physical substructure, which is the actuator in this test, is supposed to synchronise both the outputs of the two substructures. In doing so, the actuator can behave as if it was a pre-defined system in the numerical substructure, driven by the system excitation.

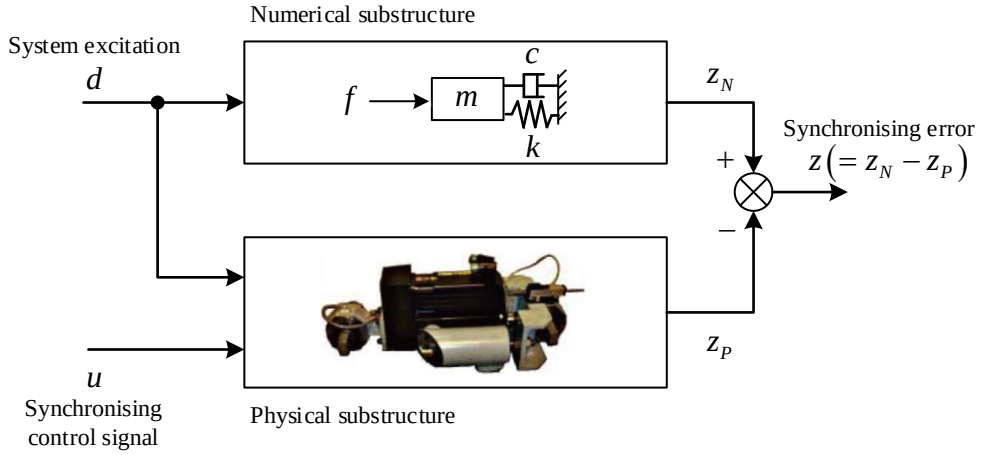

Figure 12. DSS structure of the test.

3.2. System identification and control design

System identification of the actuator was conducted via the transfer function estimation method using a uniformly distributed random input, (u in Figure 12), resulting in the transfer function gain from u

to z_P as shown in Figure 13(a). This indicates that the transfer function has approximately the characteristics of an integrator in the low frequency range (the corresponding phase was also approximately -90° over this range) and can be modelled as:

$$\Sigma_P(s) \simeq \frac{12}{s} \tag{14}$$

The associated uncertainty can be quantified as the following additive term:

$$\tilde{\Sigma}_P(s) = \Sigma_P(s) + \Delta(s) W_\Delta(s), \quad \|\Delta\|_\infty \le 1 \tag{15}$$

where $W_\Delta(s)$ can be chosen to cover the likely uncertainty over the entire frequency range, thus:

$$W_\Delta(s) = \frac{30(s+1000)^4(s+30)}{(s+5000)^4(s+10^{-4})} \tag{16}$$

The gain plot of $W_\Delta(s)$ and the additive error between the measured and identified transfer gain of Σ_P are shown in Figure 13(b).

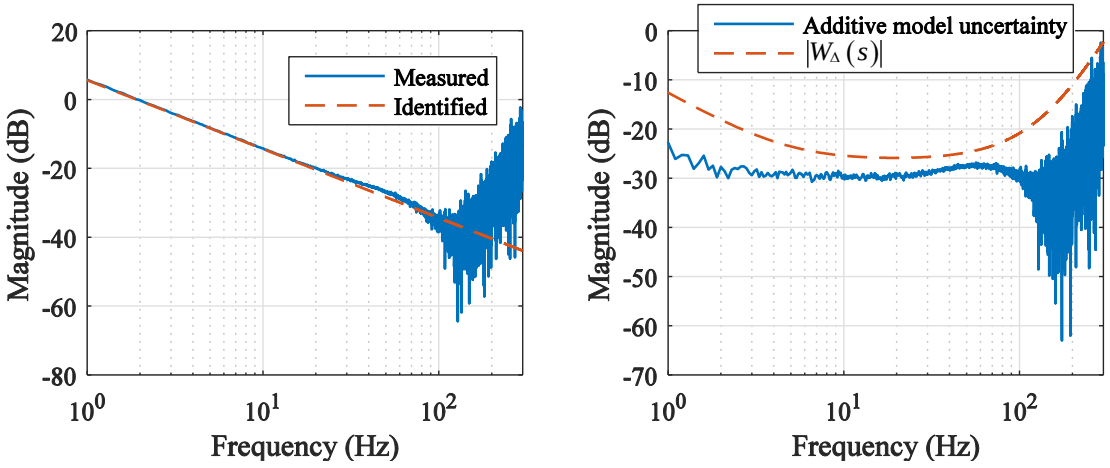

(a) (b)

Figure 13. System identification results for the physical substructure.

As a consequence, the control specification could be defined by the following weighting function:

$$W_z(s) = \frac{1.8\times10^{10}}{(s+10^{-4})(0.03s+1)^2} \tag{17}$$

Equation (17) demands that the transfer function gain $|z(s)/d(s)|$ is less than $|1/W_z(s)|$ over all frequencies.

Using the defined control specification and uncertain model set, the DSS generalised plant is shown in Figure 14, where the system, Σ_C, is identical to the physical plant, Σ_P. Since the numerical plant has no model uncertainty, it is preferable to assign Σ_P and Σ_N separately; in this case, Σ_N is assigned as W_N in Figure 14.

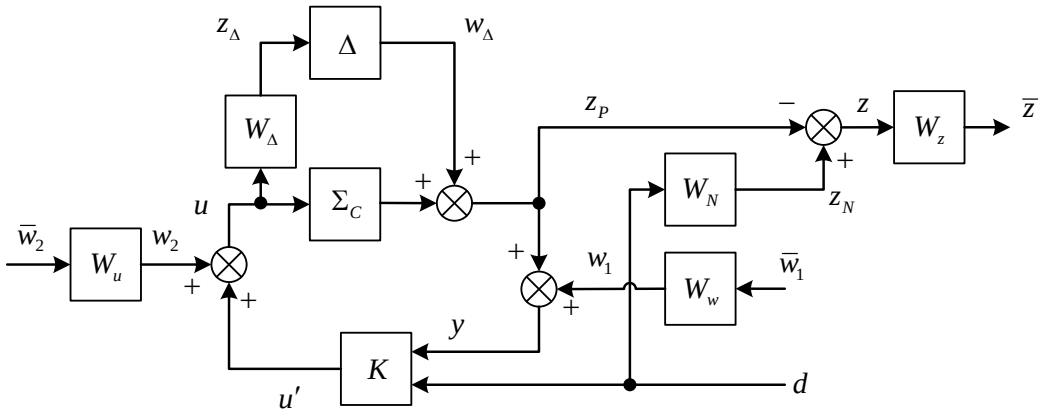

Figure 14. Generalised plant of the DSS.

Choosing $m = 0.5\,\text{kg}$, $k = 6.0\times10^7\,\text{N/m}$ and $c = 6.0\times10^4\,\text{Ns/m}$, W_N, which is identical to Σ_N, can now be expressed as:

$$W_N(s) = \frac{1}{0.5s^2 + 6.0\times10^4 s + 6.0\times10^7} \tag{18}$$

and the weighting functions that specify input and observation noise processes were chosen as:

$$W_u(s) = 10^{-8},\ W_w(s) = 5.6\times10^{-8} \tag{19}$$

Using the D-K iteration, a controller was found that satisfied the following condition on the structured singular value:

$$\sup_{\omega\in\mathbb{R}} \mu_{\Delta_P}\left(M_{\bar{z}z\Delta,d\bar{w}_1\bar{w}_2w\Delta}(j\omega)\right) \le 1 \tag{20}$$

where $M_{\bar{z}z\Delta,d\bar{w}_1\bar{w}_2w\Delta}(s)$ is the transfer function matrix relating $(d,\bar{w}_1,\bar{w}_2,w_\Delta)$ to $(\bar{z},z_\Delta)$ in Figure 14 and Δ_P is the appropriately redefined matrix in a manner similar to (11). As a result, the designed control performance is theoretically guaranteed for all possible models out of the uncertain model set, the quantified input and the observation noise. This theoretical assertion will be seen to be supported by the experimental results in the next section.

3.3. Experimental results

In order to confirm the designated control performance, the following experiment was conducted. Instead of applying the actual force to the actuator, pre-recorded uniform random signal was applied as an external disturbance. The corresponding test result is shown in Figure 15. The transfer gain between the external disturbance and the synchronising error is displayed in Figure 15(a), where the designed synchronising performance was surely satisfied. The time series of the external disturbance, both outputs of the numerical/physical substructures and the synchronising error are depicted in Figure 15(b), (c) and (d), respectively.

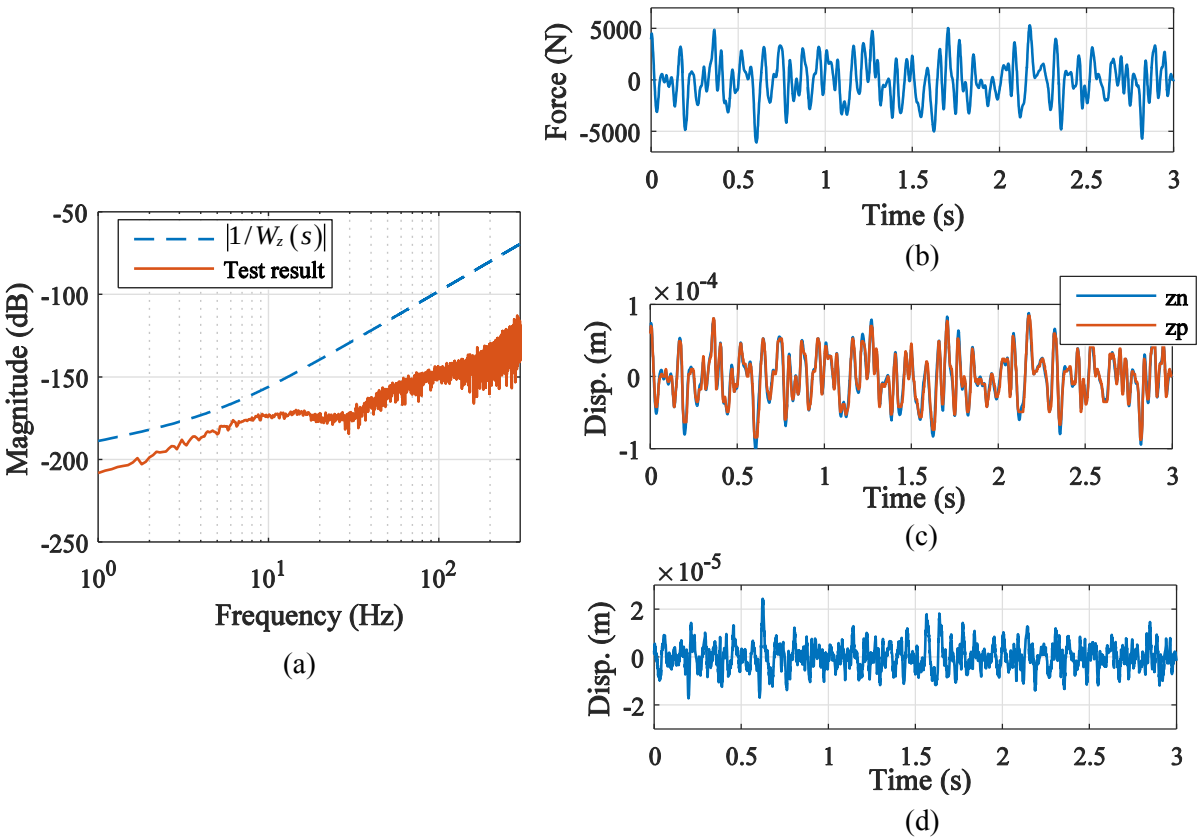

Figure 15. DSS test results
(a) transfer function gain of z/d; (b) disturbance d; (c) substructure outputs, $\{z_N, z_P\}$; (d) synchronisation error, z.

4. Conclusions and further work

In this paper, a systematic state-space approach was provided for the design of a 2-DOF output-feedback controller for DSS. Using this approach, the explicit derivation of a FF controller and a state observer was avoided, by utilising a trade-off between certain practical requirements such as the synchronising performance and the input limitations of actuators. The derived controller also guaranteed robust performance via the use of standard results from H_∞ / μ control theory. In addition, experimental work validated the efficacy of the developed method. Further work will include an application to a railway testing facility at Railway Technical Research Institute (RTRI, Tokyo), brief details being given in the following section.

4.1. Application for railway testing facility (rapid prototyping bogie)

In order to apply the DSS technique and the proposed method of design into a more practical system, a railway testing vehicle, called as a rapid prototyping bogie (RPB, [10]) will be examined. In the field of railway vehicle dynamics, the running gear - often referred to as a bogie - plays a significant role in ensuring safety and passenger comfort in railway vehicles [11]. The RPB has several electric actuators that emulate vital railway components (e.g. rubber bush, oil damper, active controlled device, etc.) instead of installing each passive component (Figure 16). This enables us to accelerate the efficiency of the bogie designing process, optimising each parameter employing the RPB as a “running test bed”.

The concept of the RPB problem and the corresponding DSS design is quite similar to what is described in §3, where the actuator now emulates a certain component that is driven by an external force. The actuators installed in the RPB also have strain gauges, which measure an external force to drive the numerical substructures.

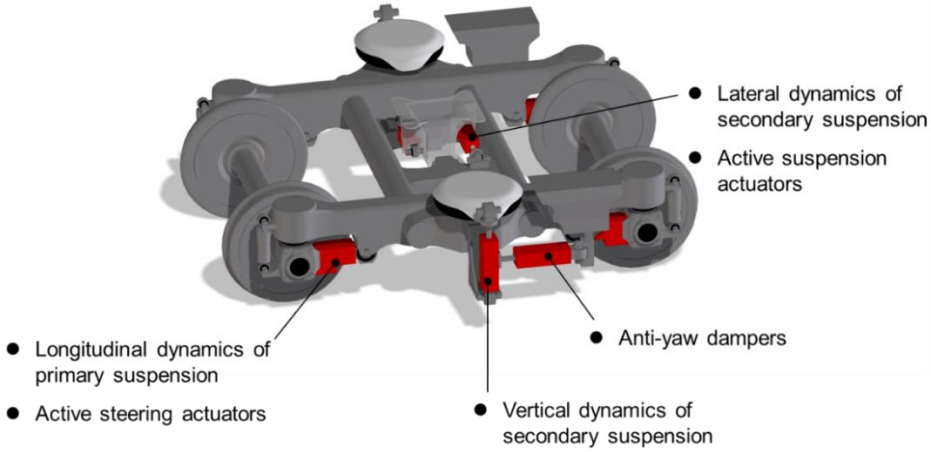

Figure 16. Rapid prototyping bogie; actuators shown in red and the listed dynamics are emulated by the corresponding actuators.

Acknowledgements
The authors gratefully acknowledge the funding from the Department of Mechanical Engineering at the University of Bristol and the Railway Technical Research Institute.

References

[1] Stoten D P and Hyde R A 2006 Adaptive control of dynamically substructured systems: the single-input single-output case *Proc. IMechE - Part I: Journ. Sys. Cont. Eng* **220** pp 63-79
[2] Spiryagin M and Cole C 2013 Hardware-in-the-loop simulations for railway research *Vehicle System Dynamics* **51** 4 pp 497-498
[3] Bosso N and Zampieri N 2013 Real-time implementation of a traction control algorithm on a scaled roller rig *Vehicle System Dynamics* **51** 4 pp 517-541
[4] Facchinetti A, Gasparetto L and Bruni S 2013 Real-time catenary models for the hardware-in-the-loop simulation of the pantograph–catenary interaction *Vehicle System Dynamics* **51** 4 pp 499-516
[5] Stoten D P 2014 A comparison of hybrid and DSS schemes for substructured system testing *12th International Conference on Motion and Vibration – MOVIC 2014* (Sapporo, Japan, Aug. 4-6) 3D11 pp 1-12
[6] Tu J Y, Stoten D P, Hyde R A and Li G 2011 A state-space approach for the control of multivariable dynamically substructured systems *Proc. IMechE - Part I: Journ. Sys. Cont. Eng*. **225** pp 935-953
[7] Enokida R and Stoten D P 2014 Comparative results for DSS and hybrid testing for a base isolated structure with rubber bearings *12th International Conference on Motion and Vibration – MOVIC 2014* (Sapporo, Japan, Aug. 4-6) 3D15 pp 1-10
[8] Doyle J, Francis B and Tannenbaum A 1992 *Feedback control theory* (New York: Macmillan Publishing)
[9] Gu D, Petkov P H and Konstantinov M M 2013 *Robust Control Design with MATLAB* (London: Springer-Verlag)
[10] Watanabe N, Sasaki K, Koganei R and Morishita H 2012 Fundamental tests on a rapid prototype bogie *Quarterly Report of RTRI* **53** pp 199-204
[11] Iwnicki S 2006 *Handbook of railway vehicle dynamics* (Boca Raton: CRC Press)